Corrosion Behavior of Plasma-Sprayed Coatings on a Ni-Base Superalloy in Na_2SO_4-60 Pct V_2O_5 Environment at 900 °C

HARPREET SINGH, D. PURI, and S. PRAKASH

The shrouded plasma spray process was used to deposit NiCrAlY, Ni-20Cr, Ni_3Al, and Stellite-6 metallic coatings on a Ni-based superalloy (62Ni-23Cr-1.48Al-0.80Mn-0.37Si-0.10Cu-0.025C-bal Fe). NiCrAlY was used as a bond coat in all cases. Hot corrosion studies were conducted on uncoated as well as plasma-spray-coated superalloy specimens after exposure to molten salt at 900 °C under cyclic conditions. The thermogravimetric technique was used to establish the kinetics of corrosion. X-ray diffraction (XRD), scanning electron microscopy/energy-dispersive X-ray analysis (SEM/EDAX) and electron-probe microanalysis techniques were used to analyze the corrosion products. The uncoated superalloy suffered accelerated corrosion in the form of intense spalling of the scale. The NiCrAlY coated specimen showed a minimum weight gain, whereas the Stellite-6 indicated a maximum weight gain among the coatings studied. All the coatings were found to be successful in developing resistance against hot corrosion, which may be attributed to the formation of oxides, and spinels of nickel, aluminum, chromium, or cobalt.

I. INTRODUCTION

GAS turbine technology for power generation and for aero engine applications places an increasing demand on the use of high-temperature Ni-based superalloys, *e.g.*, for highly loaded turbine blades.[1] The Ni-based superalloys are well known to be susceptible to hot corrosion associated with combined reaction processes such as sulfidation-oxidation and occasionally together with chlorination. In practice, it is a serious problem for such alloy systems when used for hot section components of various heat engines such as gas turbines[2] and steam generating plants. In such environments, protective coatings on the surface of superalloys are frequently considered.

From a production point of view, three methods are in current use to obtain protective coatings: chemical vapor deposition (CVD) from a pack, physical vapor deposition (PVD), and thermal spraying. A serious drawback of the pack process is the inclusion of pack particles in the coating, which can lead to coating failure.[3] Moreover, a disadvantage of the CVD process is that, because it is a non-line-of-site technique, proper masking and tooling become design considerations and an expense.[4] As far as the PVD method is concerned, it is a complex process, especially in the case of deposition of M-Cr-Al-Y type coatings, as the vaporization pressures of each of the elements of interest must be considered in producing controlled alloy chemistry. Still, vapor deposition (a diffusion process) and plasma spray (a thermal spray process) have been reported to be two major coating processing technologies used worldwide.[4] Further, the thermal spray coatings often have superior properties with lower application cost and less environmental hazards as and when compared to other industrially used coatings such as CVD, PVD, and hard chromium plating. Further, as the temperature of the gas turbines is increased, it becomes impossible to achieve the service lives using the diffusion coatings.[5]

Plasma spraying is a versatile technology that has been successful as a reliable cost-effective solution for many industrial problems.[6] The advanced plasma technique has many advantages such as high productivity for thick coating films of more than 100-μm and good applicability for a wide range of coating materials including ceramic powder. Furthermore, the process does not cause degradation of the mechanical properties of the alloy substrate.[7,8]

Overlay coatings in general pertain to all types of nondiffusional surface treatment processes where a film or a coating is deposited on top of a substrate. One particular area where the overlay coatings are considered is corrosion-resistant alloys specially designed for high-temperature surface protection. They are often referred to as M-Cr-Al-Y coatings, where M is the alloy base metal (typically nickel, cobalt, or a combination of these two).[9] The high resistance of high-chromium, nickel-chromium alloys to high-temperature oxidation and corrosion makes them widely used as welded and thermally sprayed coatings in fossil fuel–fired boilers, waste incineration boilers, and electric furnaces.[10]

Nickel aluminide has been claimed to possess high-temperature mechanical strength, as well as oxidation resistance.[11,12] Nickel aluminide-type coatings are not a very old concept. Chuanxian *et al.*[13] and Liao *et al.*[14] has reported wide use of cermet (WC/Co) thermal spray coatings in wear situations because they combine several advantages such as resistance to abrasion, erosion, high temperature, and corrosive atmospheres.

The MCrAlY bond coats provide a rough surface for mechanical bonding of the ceramic top coat, protect the underlying alloy substrate against high-temperature oxidation corrosion, and minimize the effect of coefficient of thermal expansion mismatch between the substrate and the ceramic top coat materials.[15] Furthermore, they play a role in formation of metallurgical bonds between the mating surfaces.

The objective of this work is to study the high-temperature corrosion mechanisms for plasma spray metallic coatings

HARPREET SINGH, Research Scholar, D. PURI, Assistant Professor, and S. PRAKASH, Professor and Head, are with the Metallurgical & Materials Engineering Department, Indian Institute of Technology Roorkee, Roorkee-247 667, (UA)-India. Contact e-mail: hnr97@yahoo.com

Manuscript submitted June 17, 2004.

of NiCrAlY, Ni-20Cr, Ni_3Al, and Stellite-6 on a Ni-based superalloy, namely, Superni 601 (similar grade INCONEL* 601)

*INCONEL is a trademark of INCO Alloys International, Huntington Woods, WV.

in an aggressive environment of molten salt (Na_2SO_4-60 pct V_2O_5). The study has been conducted in view of the fact that there has been little discussion of high-temperature corrosion testing on thermal-sprayed coatings in the literature.[16] Further, it has been learned from the literature that due to the intrinsic properties of the thermal spraying technique, more work is needed to obtain a reliable corrosion-resistant coating in many environments.[17]

The salt mixture Na_2SO_4-60 pct V_2O_5 has been selected for the study due to the fact that the vanadium and sodium are common impurities in low-grade petroleum fuels. Molten sulfate-vanadate deposits resulting from the condensation of combustion products of such fuels are extremely corrosive to high-temperature materials in the combustion systems.[18] The Na_2SO_4-60 pct V_2O_5 is an eutectic mixture with a melting point 550 °C and provides a very aggressive environment. The cyclic conditions have been chosen to create a more aggressive situation of corrosion attack.

II. EXPERIMENTAL PROCEDURE

A. *Development of Coatings*

The substrate material selected for the study was a Ni-based superalloy, namely, Superni 601, being procured from Mishra Dhatu Nigam Limited (Hyderabad, India) in the rolled sheet form. The chemical composition of the substrate material is 62Ni-23Cr-1.48Al-0.80Mn-0.37Si-0.10Cu-0.025C-bal Fe. The specimens each measuring approximately 20 × 15 × 5 mm were cut from the sheet. The specimens were polished and grit blasted with alumina powders (grit 60) before being plasma sprayed. The coatings were then formulated on the Ni-base superalloy specimens with a 40 kW Miller thermal plasma spray gun (Miller Thermal Spray Systems, USA). All the process parameters including the spray distance were constant throughout the coating process with an arc current of 700 A; arc voltage, 35 V; powder flow rate, 3.2 rev./min; spraying distance, 90 to 110 mm; and plasma arc gas (argon) and powder carrier gas (argon) pressures of 59 and 40 psi, respectively. The details of coating powders and porosity (2 to 4.5 pct) measurement of as-sprayed coatings are reported in an earlier publication of the authors.[19] The average thickness of the coatings as measured from backscattered electron images (BSEIs) is reproduced in Table I.

Table I. Average Coating Thickness of the As-Sprayed Coatings

	Coating Thickness (μm)		
Coating	Bond Coat	Outer Coat	Total
NiCrAlY	228	—	228
Ni-20Cr	155	211	366
Ni_3Al	166	247	413
*Stellite-6	162	365	527

*Stellite is registered trademark of Haynes International.

B. *Molten Salt Corrosion Tests*

Cyclic studies were performed in molten salt (Na_2SO_4-60 pct V_2O_5) for 50 cycles. Each cycle consisted of 1 hour heating at 900 °C in a silicon carbide tube furnace followed by 20 minutes of cooling at room temperature. The specimens were kept in alumina boats and then the boats were inserted in the furnace. The aim of cyclic hot corrosion is to create accelerated conditions for testing. The studies were performed for uncoated as well as coated specimens for the purpose of comparison. The specimens were polished down to 1-μm alumina powder on a wheel cloth polishing machine before being subjected to cyclic corrosion. The coating of uniform thickness with 3 to 5 mg/cm^2 of Na_2SO_4-60 pct V_2O_5 was applied with a camel hair brush on the preheated sample (250 °C). The weight change measurements were taken at the end of each cycle with the help of electronic balance model 06120 (Contech)* with a sensitivity of 1 mg.

*CONTECH is a registered trademark of Contech Instruments Ltd., Mumbai, India.

The spalled scale was also included at the time of measurements of weight change to determine the total rate of corrosion, wherever possible. Efforts were made to formulate the kinetics of corrosion. The samples after corrosion were subjected to scanning electron microscopy/energy-dispersive X-ray analysis (SEM/EDAX) and X-ray diffraction (XRD) for analysis of corrosion products.

A scanning electron microscope (JEOL* JSM-5800) with

*JEOL is a trademark of Japan Electron Optics Ltd.

EDAX attachment of Oxford (model-6841) made in England (High Wycombe, Bucks, UK) was used for surface SEM/EDAX analysis of the hot-corroded specimens. The equipment can directly indicate the phases (oxides) present along with their compositions based on built-in EDAX soft ware, which is a patented product of Oxford ISIS300, while the XRD analysis of the hot-corroded specimens was carried out with a Bruker AXS D-8 advance diffractometer (Bruker AXS, GmbH, Karlsruhe, Germany) with Cu K_α radiation. The hot-corroded specimens were then cut across the cross sections with a ISOMET 1000 (Buehler, IL) precision diamond cutter. These cross sections were then mounted in transoptic mounting resin, mirror polished, and carbon coated to obtain X-ray mappings of the various elements present across scale with a JEOL JXA-8600M microprobe analyzer. X-ray mappings were obtained for all the elements of the substrate, the coatings, and the molten salt, but only those important from the point of view of discussion are reported to limit the size of the article.

III. RESULTS

A. *Cyclic Corrosion in Molten Salt*

The weight gain plots for the substrate superalloy without coating and with different coatings have been shown in Figure 1 in the presence of a salt layer of Na_2SO_4-60 pct V_2O_5 at 900 °C. The uncoated superalloy has shown parabolic behavior with intensive spalling during the early cycles. After the first cycle, a fragile scale could be seen on the surfaces of the specimen with cracks at the edges. The fragile scale could not sustain and started separating from the

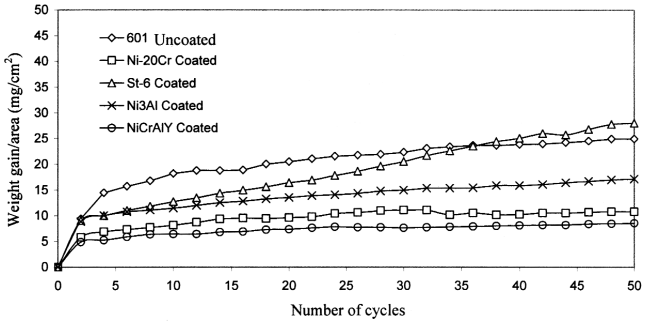

Fig. 1—Weight gain *vs* number of cycles plot for coated and uncoated superalloy Superni 601 subjected to cyclic oxidation for 50 cycles in Na_2SO_4-60 pct V_2O_5 at 900 °C.

surfaces in the form of tiny flakes, and by the end of the fourteenth cycle, almost the entire scale detached from the surfaces of the specimen. The surface of the specimen became gradually rough with progressive study, with an increasing amount of corrosion products collecting in the boat. The color of the scale was dark gray with a green tinge.

Among the coatings studied, the NiCrAlY coated superalloy has shown minimum weight gain, whereas the St-6 coated alloy showed a maximum weight gain of 3.3 times that perceived by the former. The weight gained by the NiCrAlY coated alloy is just 34 pct of that gained by the uncoated superalloy. Further the Ni-20Cr coated superalloy showed the second lowest weight gain, which is 43 pct of that indicated by the uncoated superalloy, whereas weight gain by the Ni_3Al coated alloy is 1.6 times that by the Ni-20Cr coated specimen, but still less than the weight gain by the uncoated superalloy. However, the weight gained by the St-6 coated superalloy is slightly more than the weight gained by the uncoated specimen, which is 1.12 times the latter. Figure 2 shows the cumulative weight gain/unit area for all the five cases.

The NiCrAlY, Ni-20Cr, Ni_3Al, and St-6 coatings showed cracks at the edges and spalling of the same from the edges as well as from the corners of flat surfaces of the specimens. NiCrAlY and Ni_3Al coatings showed the tendency of the cracking and spalling in the initial cycles, whereas the same phenomena were observed in Ni-20Cr and St-6 coatings in the later cycles of the study. In the case of Ni-20Cr and Ni_3Al coated superalloys, spalling of the scale was not observed, whereas in the case of NiCrAlY coatings, the same was seen from the 24th cycle onward in the form of fine greenish powder. The spalling of the scale in the case of the St-6 coating took place in the form of blackish powder from the 36th cycle onward, which was less than that shown by the uncoated superalloy. The color of scale formed in NiCrAlY, Ni-20Cr, and Ni_3Al was greenish, whereas it was dark gray in the case of the St-6 coated superalloy.

Figure 3 shows a (weight gain/area)^2 *vs* number of cycles plot from which it can be inferred that the uncoated as well as coated superalloy specimens nearly followed the parabolic rate law so far as the corrosion kinetics is concerned. Table II shows calculated values of the parabolic rate constant K_p for the coatings studied.

B. *X-ray Diffraction Analysis*

The XRD patterns of the hot-corroded specimens after 50 cycles are shown in Figure 5 on reduced scales. The *d* values corresponding to each peak were evaluated by default by the XRD software. Analysis shows that the uncoated superalloy has $NiCr_2O_4$, Fe_2O_3, and FeV_2O_4 phases in its scale along with relatively weak peaks of NiO phase. In the scales of NiCrAlY, Ni-20Cr, and Ni_3Al coated specimens, NiO is indicated as the strongest phase. The XRD analysis for the corroded NiCrAlY coating has also confirmed the presence of Al_2O_3, while Fe_2O_3 and FeV_2O_4 phases are absent. Small quantities of $NiCr_2O_4$ are found to be present in the scale of Ni-20Cr. The scale of the Ni_3Al coated superalloy has shown some weak peaks indicating probable formation of $NiAl_2O_4$, while CoO and $CoCr_2O_4$ phases are revealed in the scale of the St-6 coated superalloy. Relatively low intensity peaks pertaining to Cr_2O_3 phase could be analyzed in all cases except the Ni_3Al scale; some peaks are visible in respective figures, whereas others could not be seen due to reduced scales.

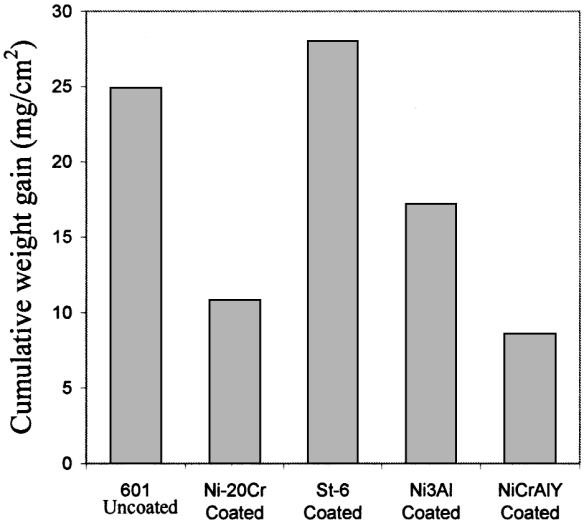

Fig. 2—Bar chart showing cumulative weight gain per unit area for the coated and uncoated superalloy Superni 601 subjected to cyclic oxidation for 50 cycles in Na_2SO_4-60 pct V_2O_5 at 900 °C.

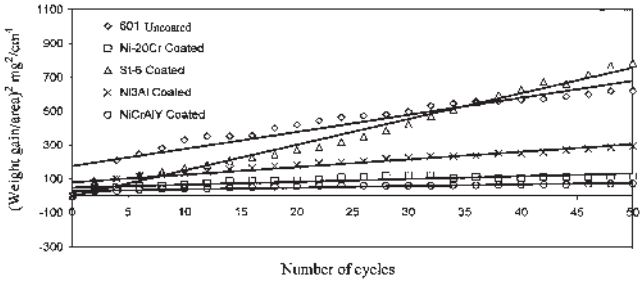

Fig. 3—(Weight gain/area)^2 *vs* number of cycles plot for coated and uncoated superalloy Superni 601 subjected to cyclic oxidation for 50 cycles in Na_2SO_4-60 pct V_2O_5 at 900 °C.

Table II. Values of the Parabolic Rate Constant K_p

Description	K_p (10^{-10} g^2 cm^{-4} s^{-1})
NiCrAlY coated	2.82
Ni-20Cr coated	4.72
Ni_3Al coated	12.63
St-6 coated	42.36
Uncoated superalloy	28.08

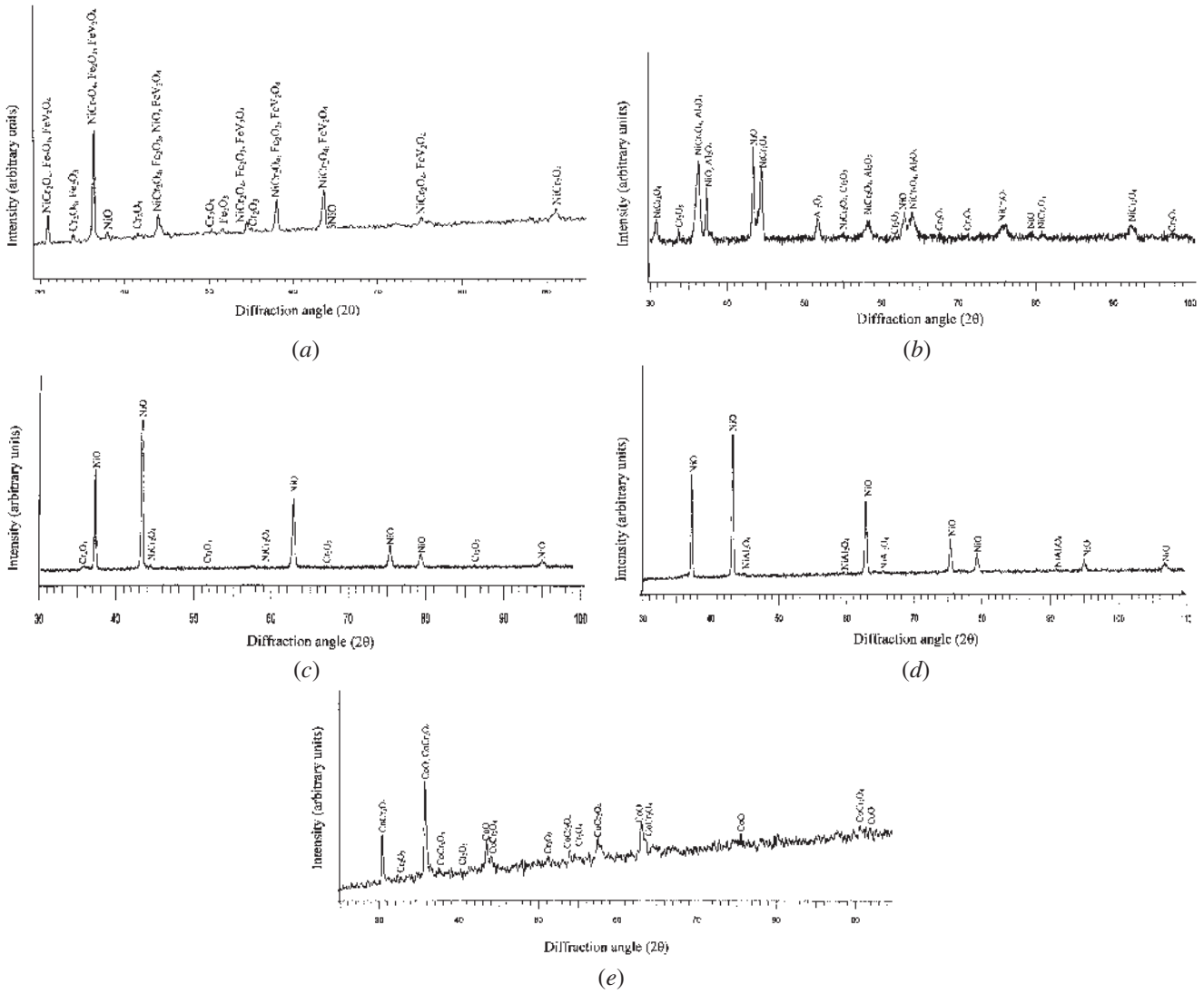

Fig. 4—X-ray diffraction patterns for the superalloy Superni 601 subjected to cyclic oxidation in Na_2SO_4-60 pct V_2O_5 at 900 °C after 50 cycles: (*a*) uncoated, (*b*) MCrAlY coated, (*c*) Ni-20Cr coated with bond coat, (*d*) Ni_3Al coated with bond coat, and (*e*) St-6 coated with bond coat.

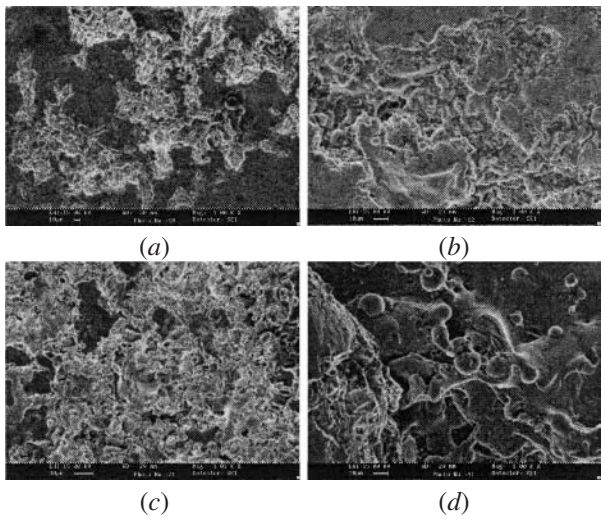

Fig. 5—SEM micrographs for plasma-sprayed coatings on superalloy Superni 601: (*a*) MCrAlY coating, (*b*) Ni-20Cr coating, (*c*) Ni_3Al coating, and (*d*) St-6 coating.

C. *SEM/EDAX Analysis*

The SEM micrographs indicating morphologies of the plasma-sprayed coatings before being subjected to hot corrosion tests are shown in Figure 5. The micrographs show the formation of typical splat structure for all the plasma-sprayed coatings in general, whereas SEM micrographs for the substrate and the coated superalloy specimens after cyclic hot corrosion for 50 cycles at 900 °C are reported in Figure 6. The EDAX analysis of the scale for the uncoated specimen has shown NiO, Cr_2O_3, and Fe_2O_3 phases. For NiCrAlY coating, the point analysis shows higher percentages of NiO and Cr_2O_3 along with a significant amount of Al_2O_3 and V_2O_5 at point 2. The EDAX of the Ni-20Cr coating scale indicates the dominance of the NiO phase with small quantities of Al_2O_3, Cr_2O_3, and V_2O_5 at point 1. The scale of the Ni_3Al coated specimen has been found to be similar in composition to the scale of the Ni-20Cr coated with a small quantity of Na_2O at point 2. The EDAX analysis of the St-6 coated superalloy scale identified CoO as the main phase with a significant amount of Cr_2O_3. Small

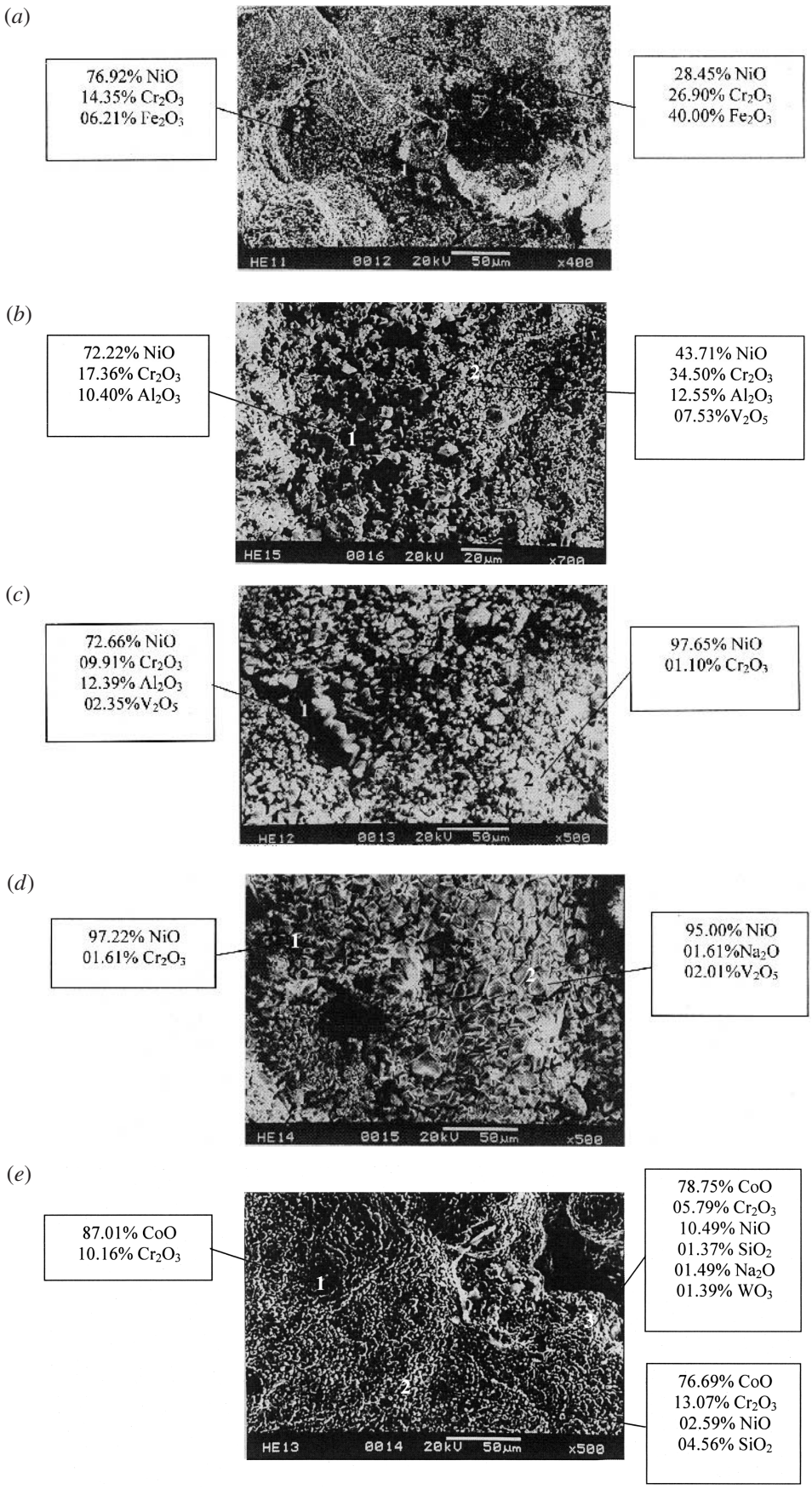

Fig. 6—Surface scale morphology and EDAX analysis for the superalloy Superni 601 subjected to cyclic oxidation in Na_2SO_4-60 pct V_2O_5 at 900 °C: (*a*) uncoated, (*b*) MCrAlY coated, (*c*) Ni-20Cr coated with bond coat, (*d*) Ni_3Al coated with bond coat, and (*e*) St-6 coated with bond coat.

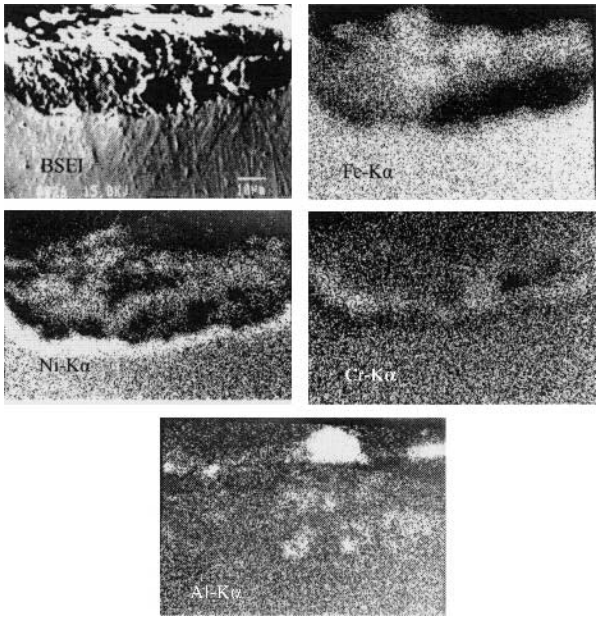

Fig. 7—Composition image (BSEI) and X-ray mapping of the cross section of the uncoated superalloy Superni 601 subjected to cyclic hot corrosion at 900 °C in Na_2SO_4-60 pct V_2O_5 after 50 cycles.

amounts of Na_2O, NiO, SiO_2, and WO_3 have also been noticed in the St-6 scale.

D. *Cross-Sectional Analysis of the Oxide Scales*

The oxide scale morphology for the uncoated superalloy after cyclic corrosion for 50 cycles is shown in Figure 7, which is a porous scale, consisting of different layers. The upper layer is rich in iron with clusters of aluminum, which also contains some nickel. The middle layer of the scale has high chromium concentration alongwith some aluminum-rich areas. Iron is absent in this layer. Nickel has shown its presence in the form of a dense layer at the scale/substrate interface.

The X-ray mappings for NiCrAlY coated superalloy indicate a top layer mainly containing aluminum, with some chromium and nickel present in it. The top layer is followed by a dense underlayer that mainly consists of chromium and nickel (Figure 8). Yttrium is found to be dispersed as clusters throughout the coat. The diffusion of the iron into the bondcoat from the substrate is also indicated.

Whereas X-ray mappings of the oxidized Ni-20 Cr coated superalloy specimen Figure 9 show a dense scale, the upper layer of the scale is rich in nickel, with an underlayer consisting of nickel and chromium. There is a Ni-rich area in the middle of the scale where Cr is depleted, which indicates that crack might have formed and become heeled by diffusion of Ni from the bond coat. Aluminum has diffused to the places where nickel and chromium are absent in the upper coat. Besides, iron and manganese showed some diffusion to the bond coat area from the substrate. Yttrium was observed to be mainly confined to the bond coat, with a minor diffusion of the same into the top coat. The presence of vanadium in the top coat as well as the bond coat was also confirmed by X-ray mappings.

The X-ray mappings for St-6 coated superalloy (Figure 10) indicate a dense layer consisting mainly of chromium and

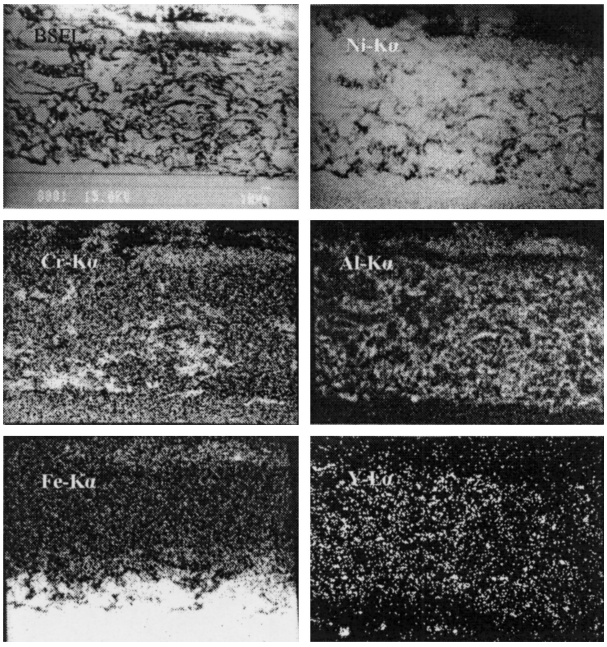

Fig. 8—Composition image (BSEI) and X-ray mapping of the cross section of the NiCrAlY coated superalloy Superni 601 subjected to cyclic hot corrosion at 900 °C in Na_2SO_4-60 pct V_2O_5 after 50 cycles.

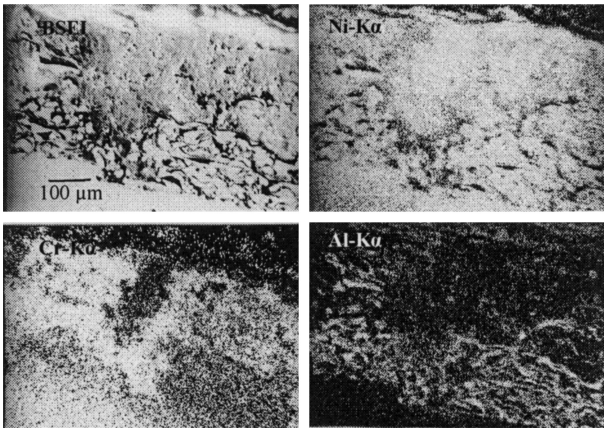

Fig. 9—Composition image (BSEI) and X-ray mapping of the cross section of the Ni-20Cr coated superalloy Superni 601 subjected to cyclic hot corrosion at 900 °C in Na_2SO_4-60 pct V_2O_5 after 50 cycles.

cobalt, which also contain tungsten and aluminum. Minor diffusion of iron into the bond coat was also noticed. The bond coat retained its identity.

IV. DISCUSSION

In general, the uncoated specimen indicated accelerated hot corrosion in the Na_2SO_4-60 pct V_2O_5 environment at 900 °C as compared to the coated specimens. A very similar weight change trend had been observed by Gitanjaly[20] for the same uncoated superalloy Superni 601. She had also reported formation of phases such as Fe_2O_3, FeV_2O_4, $NiCr_2O_4$, NiO, and Cr_2O_3 for the similar superalloy. The parabolic rate constant for the uncoated superalloy up to 50 cycles is greater than for

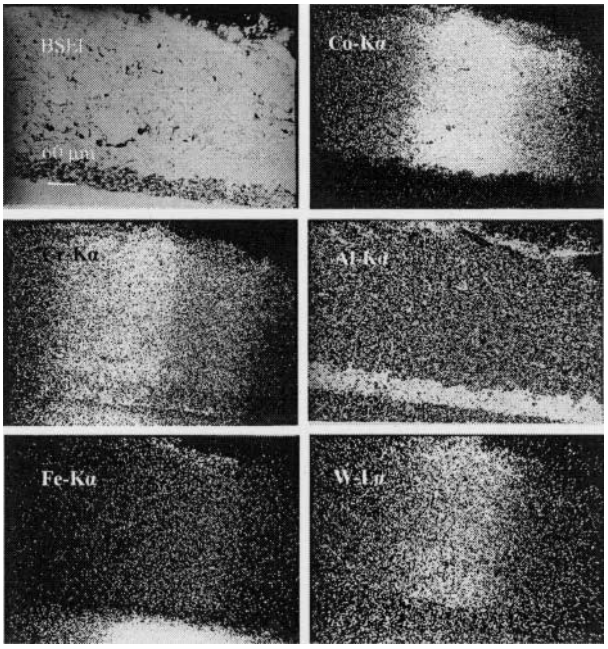

Fig. 10—Composition image (BSEI) and X-ray mapping of the cross section of the Stellite-6 coated superalloy Superni 601 subjected to cyclic hot corrosion at 900 °C in Na_2SO_4-60 pct V_2O_5 after 50 cycles.

NiCrAlY, Ni-20Cr, and Ni_3Al coatings, whereas it is smaller than that for the St-6 coating. Further, it has been observed that the spalling of the scale in the case of coated specimens is much less as compared to the one observed with the uncoated specimen. The scales formed on the coated specimens were found to be intact, whereas in the case of the uncoated specimen, the scale had poor adhesion. So, it can be inferred that necessary protection has been provided by various coatings to the substrate. Further, all the coatings resulted in parabolic oxidation behavior up to 50 cycles in the given environment.

The uncoated specimen underwent intense spalling and the weight gain was enormous. There was continuous increase in the weight, but the rate of increase was high during the initial period of exposure. The rapid increase in weight gain during initial hours has also been reported by Gitanjaly[20] during her studies on the hot corrosion behavior of the same superalloy. This rapid increase in weight gain may be due to the rapid oxygen pickup by diffusion of oxygen through the molten salt layer. At the temperature of reaction, *i.e.*, 900 °C, the Na_2 SO_4-60 pct V_2O_5 will combine and form Na VO_3 having a melting point of 610 °C, as proposed by Kolta *et al.*,[21] which acts as a catalyst and also serves as an oxygen carrier to the metal. Chromium has a high affinity for oxygen to form Cr_2O_3, and so, in the earlier stages of hot corrosion, there is a rapid increase in weight. Intensive spalling of the scale as observed can be attributed to severe strain developed because of Fe_2O_3 precipitation from the liquid phase and inter diffusion of intermediate layers of iron oxide, as has been reported by Sachs.[22] Further, the presence of three different phases in a thin layer would impose severe strain on the film, which may result in cracking and exfoliation of the scale. The cracks might have allowed the aggressive liquid phase to reach the metal substrate.[22]

The appearance of cracks in the coatings during hot corrosion studies may be attributed to different values of thermal expansion coefficients of the coatings and the substrate, as reported by Singh *et al.*,[19] Sidhu and Prakash,[23] Singh,[24] Niranatlumpong *et al.*,[25] Evans and Taylor,[26] and Wang *et al.*[27] Niranatlumpong *et al.*[25] were of the opinion that the spallation could be initiated by the rapid growth of void-like defects lying adjacent to coating protuberances, at which tensile radial stress developed during cooling as a result of the thermal contraction mismatch between the oxide and the coating was maximum. The formation of cracks in the coating originates from stresses developed in the deposit or at the coating-base metal interface.[28] Through these cracks, the corrosive environment can quickly reach the base metal and cut its way under the coating to result in adhesion loss and spalling, whereas some elements may diffuse outward through these cracks to form their oxides or spinels, as has been revealed by XRD and EDAX analysis. Further, the greenish color of the scale in the case of NiCrAlY, Ni-20Cr, and Ni_3Al coated specimens may be attributed to the presence of NiO as a dominating phase in the scale identical to the findings of Singh[24] and Bornstein *et al.*[29] Further, in the case of St-6 coating, the main phase is CoO, which may contribute to the dark gray color of the scale.

NiCrAlY has provided the best protection to the base alloy, which may be attributed to the presence of $NiCr_2O_4$ spinel and oxides of nickel, aluminium, and chromium, as indicated by the XRD and EDAX analysis. X-ray mappings also support the formation of these phases (Figure 8). Singh *et al.*[19] Singh,[24] Wu *et al.*[30] and Wu (X) *et al.*[31] have also reported the formation of similar phases. Further Longa and Takemoto[32] have also identified a similar phase for NiCrAl flame-sprayed coatings on steel substrates when oxidized in an environment of Na_2SO_4-85 pct V_2O_5 at 900 °C. Seiersten and Kofstad,[33] while studying the effect of SO_3 on vanadate-induced hot corrosion of air-plasma-sprayed and electron beam (EB)-PVD NiCrAlY coatings on INCONEL 600, noticed that NiO was formed at the outer surface of the continuos oxide layer formed at 800 °C. The high percentage of nickel oxide as observed by XRD in the current study is in good agreement with the observation of Seiersten and Kofstad.[33] Further, the better protection given by the spinel phases is due to the fact that the spinels of the mixed oxides of the general composition AB_2O_4 (A and B represent two metallic components) have much smaller diffusion coefficients of the cations and anions than those in their parent oxides.[34]

The Ni-20Cr coated alloy has also shown formation of NiO as a main phase along with other oxides such as Cr_2O_3 and $NiCr_2O_4$, which are in accordance with the findings of Singh *et al.*,[19] Singh,[24] Longa-Nava *et al.*,[35] Calvarin *et al.*[36] and Nickel *et al.*[37] Calvarin *et al.*[36] have established that the oxide scale formed after high-temperature oxidation of Ni-20Cr foils at 900 °C consists of an outer NiO layer, an inner layer of Cr_2O_3, and an intermediate layer composed of oxides rich in nickel and chromium. Further, Longa-Nava *et al.*[35] have concluded from the studies on low-pressure plasma-sprayed Ni-20Cr coatings that the formation of chromate solute anions can prevent sulfidation of the alloy.

The hot corrosion resistance shown by Ni_3Al coating is inferior to that shown by NiCrAlY and Ni-20Cr coatings, whereas it performed better than St-6 coating. Ni_3Al has been reported to be a NiO former by McCarron *et al.*[38] Further,

according to Natesan,[39] the corrosion of Ni_3Al at 900 °C and above produces scales containing an outer layer of NiO, an inner layer of Al_2O_3, and an intermediate layer of the Ni-Al spinel $NiAl_2O_4$. In the current study, the same has been observed as nickel oxide (NiO) is revealed to be the main constituent from the XRD and EDAX analysis with a comparatively lesser amount of $NiAl_2O_4$. Sidhu and Prakash[23] and Malik *et al*.[40] also reported NiO phase in their studies on Ni_3Al coatings on boiler steels. The presence of $NiAl_2O_4$ and NiO was also noticed by Lee and Lin[41] during their hot corrosion studies on Ni_3Al intermetallic compounds at 800 °C and 1000 °C and by Singh *et al*.[19] According to Lee and Lin,[41] there are two possibilities of the formation of spinel phase: through the reaction of Al and Ni with oxygen in the molten salt or through the evolution of sulfides. Further, they opined that the $NiAl_2O_4$ might have provided better hot corrosion resistance than NiO, since the solubility of $NiAl_2O_4$ spinel is thermodynamically lesser than that of NiO in the molten salt. In the present study, the probable presence of the spinel has been supported by XRD analysis.

The St-6 coating has shown the least resistance to molten salt oxidation among the coatings studied. The formation of phases CoO, $CoCr_2O_4$, and Cr_2O_3 revealed by XRD and EDAX is in accordance with the studies of Singh *et al*.,[19] Singh,[24] Santoro,[42] and Luthra.[43] The protection shown by this coating may be due to the formation of oxides of cobalt and chromium, and spinel containing chromium and cobalt. Luthra[43] proposed that the formation of spinels might stop the diffusion activities through the cobalt oxide (CoO), which in turn suppresses the further formation of this oxide. He further opined that increases in the growth of $CoCr_2O_4$ and Cr_2O_3 in competition with CoO and Co_3O_4 formation increase the corrosion resistance of alloys.

Comparison with Other Methods

The corrosion resistance of a coating depends to a great extent on the rate of protective scale formation in a particular environment. According to Hocking *et al*.,[44] a major problem in hot corrosion is the formation of molten metal/metal sulfide eutectics, and so coating alloys are formulated to avoid this. They opined that interdiffusion plays an important role, as coalescence of consequent Kirkendall voids reduces coating adhesion and causes coating failure by substrate parting. They further proposed the failure mechanism of an aluminide coating as follows.

At first, Al in the aluminide coating diffuses into the substrate, but later, the diffusion direction reverses and Ni from the substrate starts to enter the coating. This creates Kirkendall voids and their coalescence can cause coating disbondment. At first, nonprotective gamma alumina forms and spalls, but then a denser adherent and protective alpha alumina forms. However, a damage and repair cycle cause Al depletion in the NiAl below the oxide and may cause precipitation of Ni_3Al, which causes NiO to form and to react with alumina to form spinels. The NiO also develops porosity during growth. The appearance of the gamma-prime phase thus marks the onset of a rapid oxidation stage. Further, if Al diffusion toward the substrate is arrested, the aluminide coating is an effective barrier for hot corrosion. That is why the aluminide coating is rarely used alone and dual systems such as Ni-Al, Co-Al, Cr-Al, or Pt-Al, or more complex systems with four to six elements, are used to resist hot corrosion, such as MCrAlX type. Moreover, increased thickness aluminides have low ductility and may modify substrate mechanical properties, thereby limiting the coating thickness for diffusion coatings. According to Sidky and Hocking,[45] diffusion aluminide coatings on superalloys lack ductility and spall at temperatures below 750 °C. That is why use of the simple aluminide coatings in applications where hot corrosion was the primary problem generally led to unsatisfactory results.[46]

In contrast, overlay coatings can be deposited thicker than diffusion coatings; thus, if they corrode at the same rate, overlay coatings will last proportionally longer than their diffusion counterparts.[47] Moreover, field experience with some early-generation MCrAlY coatings has shown long-time performance at least less equivalent to that of the platinum-aluminide coatings in terms of rate of attack

MCrAlX coatings deposited by EB-PVD are more protective than the plasma-sprayed versions, but a high vacuum is required and the process is limited to line of sight. Further, this technique is preferred for applying ceramic thermal barrier coatings for thermal insulation.[4] However, Seiersten and Kofstad[33] compared the effect of SO_3 on vanadate-induced hot corrosion of air-plasma-sprayed and EB-PVD NiCrAlY coatings on INCONEL 600. From the weight gain studies, they observed that the two types of coatings reacted at approximately the same rate when exposed to hot corrosion tests.

V. CONCLUSIONS

The plasma-sprayed coatings of NiCrAlY, Ni-20Cr, Ni_3Al, and Stellite-6 were found to be useful in developing hot corrosion resistance in a Ni-based superalloy, namely, Superni 601 in Na_2SO_4-60 pct V_2O_5 environment at 900 °C for the specified plasma-sprayed coatings.

The uncoated superalloy showed intense spalling of the scale and the weight gain was enormous during hot corrosion studies in the aggressive environment of Na_2SO_4-60 pct V_2O_5 at 900 °C.

NiCrAlY coating has provided the best protection to the base alloy, which may be due to the presence of oxides, and spinels of nickel, aluminum, and chromium in the scale. Similarly, Ni-20 Cr has shown the formation of a scale with some protective oxides such as NiO, and $NiCr_2O_4$ and Cr_2O_3 to some extent.

The hot corrosion resistance shown by the Ni_3Al coating is relatively less compared to that by NiCrAlY and Ni-20Cr coatings, whereas it performed better than the St-6 coating. The presence of the spinel $NiAl_2O_4$ and phase such as NiO might have imparted the protectiveness to the coating in the given environment.

The St-6 coating has shown the least resistance to molten salt corrosion among the coatings studied. The coating was not effective in decreasing the weight gain, although the scale was adherent and indicated less spalling.

ACKNOWLEDGMENTS

The corresponding author is grateful to Dr. D.S. Hira, Principal, BBSB Engineering College, Fatehgarh, Punjab (India) for sponsoring him to carry out this research work.

Authors are also highly indebted to Mishra Dhatu Nigam Ltd., Hyderabad (India) for providing superalloys required for the current work.

REFERENCES

1. M.F. Stroosnijder, R. Mevrel, and M.J. Bennett: *Mater. High Temp*., 1994, vol. 12 (1), pp. 53-56.
2. M. Yoshiba: *Corr. Sci*., 1993, vol. 35 (5–8), pp. 1115-24.
3. K.N. Strafford, P.K. Datta, and C.G. Googan: *Coatings and Surface Treatment for Corrosion and Wear Resistance*, Institution of Corrosion Science and Technology, Birmingham, United Kingdom, Ellis Horwood Limited, Chichester, United Kingdom, 1984.
4. J.T. DeMasi-Marcin and D.K. Gupta: *Surf. Coating*, 1994, vols. 68–69, pp. 1-9.
5. Y. Itoh, M. Saitoh, and Y. Ishiwata: *J. Eng. Gas Turbines Power (Trans. ASME)*, 2002, vol. 124, pp. 270-75.
6. P. Fauchais, J.F. Coudert, and M. Vardelle: *J. Phys*., 1997, vol. IV7, pp. C4-187-C4198.
7. B.J. Gill and R.C. Tucker, Jr.: *Mater. Sci. Technol*., 1989, vol. 2, p. 207.
8. A.R. Nicoll, H. Grruner, G. Wuest, and S. Keller: *Mater. Sci. Technol*., 1986, vol. 2, p. 214.
9. N. Eliaz, G. Shemesh, and R.M. Latanision: *Eng. Failure Analysis*, 2002, vol. 9, pp. 31-43.
10. J. Tuominen, P. Vuoristo, T. Mantyla, S. Ahmaniemi, J. Vihinen, and P.H. Andersson: *J. Thermal Spray Technol*., 2002, vol. 11 (2) pp. 233-43.
11. J.L. He, K.C. Chen, C.C. Chen, A. Leyland, and A. Matthews: *Surf. Coating Technol*., 2001, vol. 135, pp. 158-65.
12. J.H. Schneibel and P.F. Becher: *J. Chin. Inst. Eng*., 1999, vol. 22 (1), pp. 1-12.
13. C. Chuanxian, H. Bingtang, and L. Huiling: *Thin Solid Films*, 1984, vol. 118 (4), pp. 485-93.
14. H. Liao, B Normand, and C. Coddet: *Surf. Coating Technol*., 2000, vol. 124, pp. 235-42.
15. A.N. Khan and J. Lu: *Surf. Coating Technol*., 2003, vol. 166, pp. 37-43.
16. M.A Uusitalo, P.M.J. Vuoristo, and T.A Mantyla: *Mater. Sci. Eng. A, (Struct. Mater.: Prop., Microstr. and Processing)*, 2003, vol. A346 (1–2), pp. 168-77.
17. T. Hodgkiess and A Neville: *Proc. 15th Int. Thermal Spray Conf*., Nice, 1998, pp. 63-68.
18. Y.S. Hwang and R.A. Rapp: *Corrosion,* 1989, vol. 45 (11), pp. 933-37.
19. H. Singh, D. Puri, and S. Prakash: *Surf. Coating Technol*., 2005, vol. 192, pp. 27-38.
20. Gitanjaly: Ph.D. Thesis, IITR, Roorkee, India, 2003.
21. GA. Kolta, I.F. Hewaidy, and N.S. Felix: *Thermochim. Acta*, 1972, vol. 4, pp. 151-64.
22. K. Sachs: *Metallurgia*, 1958, April, pp. 167-73.
23. B.S. Sidhu and S. Prakam: *Surf. Coating Technol*., 2003, vol. 166, pp. 89-100.
24. B. Singh: Ph.D. Thesis, IITR, Roorkee, India, 2003.
25. P. Niranatlumpong, C.B. Ponton, and H.E. Evans: *Oxid Met*., 2000, vol. 53 (3–4), pp. 241-58.
26. H.E. Evans and M.P. Taylor: *Oxid Met*., 2001, vol. 55 (1–2), pp. 17-34.
27. B. Wang, J. Gong, A.Y. Wang, C. Sun, RF. Huang, and L.S. Wen: *Surf. Coating Technol*., 2002, vol. 149 (1), pp. 70-75.
28. G.R Heath, P. Heimgartner, G. Irons, R. Miller, and S. Gustafsson: *Mater. Sci. Forum*, 1997, vols 251–254, pp. 809-16.
29. N.S. Bornstein, M.A. Decrescente, and H.A. Roth: *Proc. Conf. on Gas Turbine Materials in the Marine Environment*, MMIC-75-27, Columbus, OH, 1975, pp. 115-60.
30. Y.N. Wu, G. Zhang, Z.C. Feng, B.C. Zhang, Y. Liang, and F.J. Liu: *Surf. Coating Technol*., 2001, vol. 138, pp. 56-60.
31. X. Wu, D. Weng, Z. Chen, and L. Xu: *Surf. Coating Technol*., 2002, vol. 140, pp. 231-37.
32. Y. Longa and M. Takemoto: *Corrosion*, 1992, vol. 48, pp. 599-607.
33. M. Seiersten and P. Kofstad: *High Temp. Technol*., 1987, vol. 5 (3), p. 115.
34. U.K. Chatterjee, S.K. Bose, and S.K. Roy: *Environmental Degradation of Metals*, Marcel Dekker, New York, NY, 2001.
35. Y. Longa-Nova, Y.S. Zhang, M. Takemoto, and R.A. Rapp: *Corrosion*, 1996, vol. 52 (9), pp. 680-89.
36. G. Calvarin, R. Molins, and A.M. Huntz: *Oxid Met*., 2000, vol. 53 (1–2), pp. 25-48.
37. H. Nickel, W.J. Quadakkers, and L. Singhieser: *Anal. Bioanal. Chem*., 2002, vol. 374, pp. 581-87.
38. R.L. McCarron, N.R. Lindliad, and D. Chatterji: *Corrosion*, 1976, vol. 32 (12), pp. 476-81.
39. K. Natesan: *Oxid Met*., 1988, vol. 30, p. 53.
40. A.U. Malik, R Ahmad, S. Ahmad, and S. Ahmad: *Prakt. Metallogr*., 1992, vol. 29, pp. 255-68.
41. W.H. Lee and R.Y. Lin: *Mater. Chem. Phys*., 2002, vol. 77, pp. 86-96.
42. G.J. Santoro: *Oxid Met*., 1979, vol. 13 (5), pp. 405-35.
43. K.L. Luthra: *J. Electrochem. Soc*., 1985, vol. 132 (6), pp. 1293-98.
44. M.G. Hocking, V. Vasantasree, and P.S. Sidky: *Metallic & Ceramic Coatings*, Longmans, United Kingdom, 1989.
45. P.S. Sidky and M.G. Hocking: *Br. Corr. J*., 1999, vol. 34 (3), pp. 171-83.
46. F.S. Petit and G.W. Goward: in *Coatings for High Temperature Applications*, E. Lang, ed., Applied Science Publishers, New York, 1983, p. 79.
47. J.R Nicholls: *JOM*, 2000, Jan., pp. 28-35.